

## Renewable Hybrid Stand-Alone Telecom Power System Modeling and Analysis

**Y.Hazarathaiah, M.Tech**

Assistant Professor,  
Department of EEE,

G.Pullaiah College of Engineering & Technology,  
Kurnool.

**M.Venkateswarlu, M.Tech**

Sr.Assistant Professor  
Department of EEE,

G.Pullaiah College of Engineering & Technology,  
Kurnool.

### **Abstract:**

*At the telecom service providers' installations, the problem of poor grid electricity supply is tackled by using diesel generators. These generators, however, entail a major problem in transportation and storage of diesel with noise pollution. Decentralized distributed generation technologies based on renewable energy resources such as Solar Photo Voltaic (SPV) or/and Wind Turbine Generators (WTG) address the above barriers to a large extent and are therefore considered as emerging alternate power solutions to telecommunication base stations. Three stand-alone SPV power systems using different energy storage technologies i.e. SPV-Battery system, SPV-Fuel Cell (FC) system and SPV-FC-Battery system are optimized, analyzed and compared in this paper. The modeling and sizing optimization of such hybrid systems feeding a stand-alone DC load at a telecom base station has been carried out using HOMER software. SPV system configurations with tracker are also included. Based on the simulation results, it is observed that SPV-FC-Battery hybrid system with maximum power point tracker is most economic solution compared to single storage system. Cost and energy sensitivity with solar radiation data are also analyzed in this paper.*

### **INTRODUCTION**

With expected reduction in the component cost and gain in the system performance, attention towards renewable energy alternatives for electric power generation in stand-alone applications is gaining momentum all over the world. Solar Photo Voltaic (SPV) and Wind Turbine Generators (WTG) technologies are the forerunners

amongst various types of renewable sources. However, they have a major drawback of inability to guarantee reliable, uninterrupted output at costs that can be comparable to conventional power generation. Therefore, a number of off-grid hybrid systems have been installed and tested in the past few decades. The results in literature clearly show that, renewable energy based stand-alone hybrid energy systems can compete with power from the grid in remote locations [1]. Solar radiation is the earth's most abundant energy source. The SPV modules convert solar radiation from the sun into electrical energy in the form of direct current. Its suitability for decentralized applications and its environment-friendly nature make it an attractive option for the telecommunication network in rural areas.

One of the major requirements, for a hybrid energy system is to ensure continuous power flow by storing excess energy from the renewable sources. Although, battery technology has reached a very suppurate stage; size, cost and disposal are the constraining factors for its use in remote stand-alone applications. Recent advancements in Fuel Cell (FC) and electrolyser technology have opened up the option for using hydrogen as an energy storage medium. A hybrid energy system based on such alternative technologies has been proved to be a feasible solution for stand-alone power generation at remote locations [2].

Some studies [3]-[5] are reported about design, optimum combination and analysis of hybrid renewable energy power generations with energy storage. Dmowski, Biczal and Kras [6] have simulated and experimented a SPV-FC

hybrid power plant for supplying telecom station in stand alone mode without interruptions and maximum interval of refueling period. An economic evaluation of a hybrid WTG-SPV-FC generation system is performed and compared with traditional hybrid energy system of battery in [7]. Alam and Gao [8] designed a hybrid WTG-SPV-FC system with fuzzy logic power flow controller and simulated using HOMER software. Economic analysis and controller simulation are not reported in this paper. A hybrid energy storage system coupled to SPV generation is evaluated in [9]. The cost of a SPV system using hydrogen storage method is optimized in [10] based on the downhill simplex method.

However, most of them do not take into account the effect of energy storage capacity on the whole system. Three stand alone SPV power systems using different hybrid energy storage technologies, namely, SPV-Battery system, SPV-FC system and SPV-FC-Battery system with and without Maximum Power Point Tracker (MPPT) technology are studied in this work. Key components including solar photovoltaic cell, fuel cell, electrolyzer, hydrogen tank and batteries are modeled in a clear way so as to facilitate the evolution of the power systems. The whole system is simulated in HOMER environment for sizing optimization which minimizes the system cost. Simulation results and sensitivity analysis are being reported in this paper.

Section II presents modeling of key components of hybrid energy system used for the analysis. In section III, HOMER simulation parameters, results and analysis are illustrated. Section IV discusses the results and concludes.

### SPV Hybrid System Model Development

The SPV-FC-Battery hybrid energy system architecture simulated in HOMER is shown in Fig. 1. SPV array, FC stack and battery are connected to the same DC voltage bus. There are two main sources of energy: SPV panel and FC stack. Excess power goes to the battery bank and to the electrolyzer, which generates hydrogen for storage in the hydrogen tank for the utilization by FC in case of lack of generated power from SPV. Although the battery

is an energy storage device, it is also a source of energy when the load demands excess available energy. The SPV panel provides as much power as possible to the load. The function of the fuel cell is to supply to the load, the rest of the average power that the SPV array can not meet. The SPV panel powers the load and charges the battery through a buck converter which acts as a maximum power point tracker. A boost converter converts the low DC voltage output from the fuel cell stack to the regulated bus voltage.

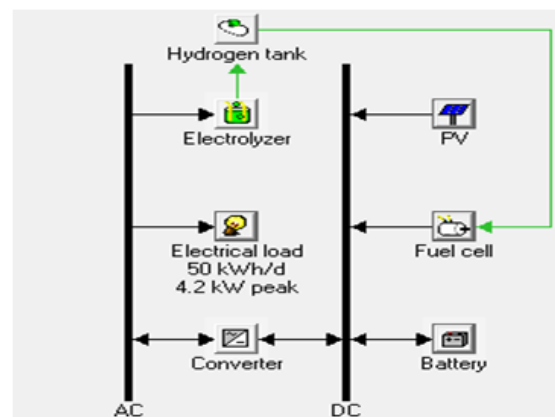


Fig. 1. SPV-FC-Battery hybrid system configuration

The battery supplies transient power to peak load demands or absorbs transient power from the main sources. The battery is directly connected to the voltage bus. The power may flow through the battery in both directions. The power conditioning system (including power converters and associated control electronics) that controls the power flowing from each source of energy are not shown in this figure.

### Solar Photovoltaic (SPV) Cell

A solar cell module is the basic element of each SPV system, which converts the sun's rays or photons directly into electrical energy. It consists of many jointly connected solar cells. A number of solar cell models have been developed, but the one diode electrical equivalent circuit [11] shown in Fig. 2 is commonly used for cell based or module based analysis. It consists of a diode, a current source, a series resistance and a parallel resistance. As a function of voltage, the current of a cell is defined by

$$I_{PV} = I_{ph} - I_D \left[ \exp\left(\frac{V_{PV} + R_s \times I_{PV}}{V_t}\right) - 1 \right] - \frac{(V_{PV} + R_s \times I_{PV})}{R_p} \quad (1)$$

where  $I_{ph}$  is the short circuit current,  $I_D$  is the diode reverse saturation current,  $V_t$  is the thermal voltage,  $R_s$  and  $R_p$  are the series and parallel resistances respectively, and  $I_{PV}$  and  $V_{PV}$  are the output current and voltage.

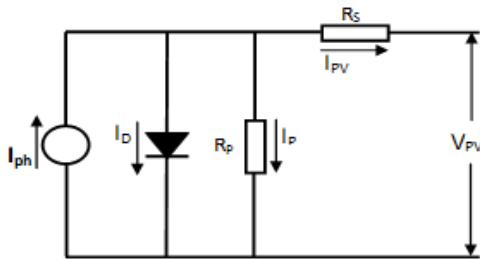


Fig. 2. SPV Cell equivalent circuit

The current source generates the photo-current that is a function of the incident solar cell radiation and temperature [6]. The diode represents the p-n junction of a solar cell. In real solar cells, a voltage drop at the external contacts is observed. This voltage drop is expressed by a series resistance ( $R_s$ ). Furthermore, leakage currents are represented by a parallel resistance ( $R_p$ ).

The output power of the solar cell increases with an increase in solar radiation and decreases with an increase in temperature. There is a unique maximum power point on I-V characteristic curve of a SPV cell as shown in Fig. 3. In order to use the most of the available solar energy, the maximum power point can be tracked using a MPPT.

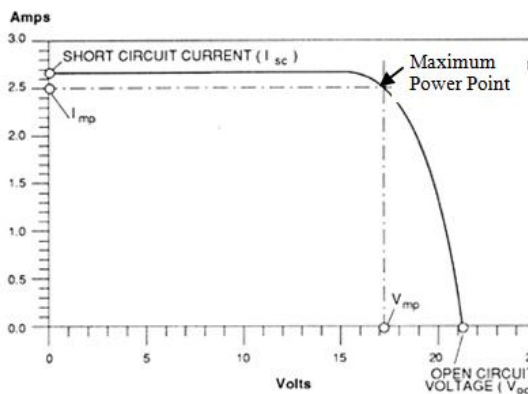
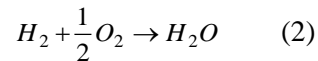


Fig. 3. I-V characteristic curve of SPV cell

### Fuel Cell (FC)

FC appears today in several configurations, operating on different electrolytes and presenting different power ranges, efficiencies and operation characteristics [12]. Proton Exchange Membrane (PEM) FC poses a good start up and shut down performance. In application upto ~100kW, it may be the most suitable choice among all kinds of FCs [13]. The fundamental structure of a PEM FC can be represented as two electrodes (anode and cathode) separated by a solid membrane. Hydrogen fuel is fed continuously to the anode and air is fed to the cathode. The overall chemical reaction is as follows



The Hydrogen consumption at rated power  $P_{FC}$  kW of FC in 1h can be calculated by

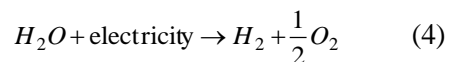
$$HY_{FC} = \frac{P_{FC} \times 3600}{2 \times V_{FC} \times F} \quad (\text{mol/h}^{-1}) \quad (3)$$

Where  $HY_{FC}$  is the amount of hydrogen consumed by FC,  $P_{FC}$  and  $V_{FC}$  are the output power and voltage of FC and  $F$  is Faraday constant [14].

In this model, FC works as back-up when renewable sources are not in a position to provide the required power and batteries are also discharged to very low levels.

### Electrolyzer

Hydrogen can be produced by the decomposition of water into its elementary components by passing the electric current. A water electrolyzer consists of several cells connected in series. Two electrodes of the electrolyzer are separated by an aqueous electrolyte or solid polymer electrolyte. Electrical current through the electrolyzer enables the decomposition of water into hydrogen and oxygen. This chemical process can be expressed by



For starting up the electrolyzer to produce hydrogen, the working voltage between its two electrodes must be higher than a minimum decomposition voltage defined by [14]

$$V_H = \frac{-\Delta h}{2F} \quad (5)$$

Where  $\Delta h(kJ/mol)$  is the high heat value of hydrogen.

According to Faraday's law, the amount of hydrogen produced by rated power of  $P_{FC}$  kW electrolyzer in 1 h can be calculated by

$$HY_{ELYZ} = \frac{P_{ELYZ} \times 3600}{2 \times V_{ELYZ} \times F} \quad (mol/h^{-1}) \quad (6)$$

Where  $HY_{ELYZ}$  is the amount of hydrogen produced by the electrolyzer, and  $P_{ELYZ}$  is the rated power of the electrolyzer and  $V_{ELYZ}$  is the working voltage of electrolyzer defined as the ratio of  $V_H$  and voltage efficiency of electrolyzer.

### Hydrogen Compressor Tank

Primarily, there are three different methods with variable characteristics for hydrogen storage: metal hydrides, liquefaction and high-pressure compression. As a general guideline, hydrides are suitable for small quantities of  $H_2$  (e.g. in the range of 1 kg) and when a high safety factor is required. Liquid  $H_2$  is advantageous with regard to space required and safety issues, while compression is the least complex storage method [13].

Hydrogen energy produced by the electrolyzer provides solar energy storage in excess of demand. The method of transforming the capacity unit mol of hydrogen tanks to the unit kWh is given in following equation.

$$E_{Tank} (kWh) = M_{Tank} (mol) \times 2 \times 10^{-3} \left(\frac{kg}{mol}\right) \times LHV \left(\frac{kWh}{kg}\right) \quad (7)$$

Where  $E_{Tank}$  and  $M_{Tank}$  are the size of hydrogen tank in units of kWh and mol respectively and LHV (-33kWh/kg) is the low heat value of the hydrogen.

### Battery

Battery bank is a traditional approach to store electrical energy with high efficiency. Its discharging level cannot exceed a minimum limit defined as depth of discharge. The capacity of the battery is so designed to supply the ultimate load during the non-sunlight hours i.e. during the night and also during the cloudy weather or when both SPV power is not available.

### HOMER Simulation

HOMER is an abbreviation of Hybrid Optimization Model for Electrical Renewable [15]. This micropower optimization model simulates the operation of a system by making energy balance calculations for each of the 8,760 hours in a year. For each hour, HOMER compares the electric demand in the hour to the energy that the system can supply in that hour, and calculates the flows of energy to and from each component of the system. HOMER performs these energy balance calculations and system cost calculations for each system configuration considered. Simulation results a list of all of the possible system sizes, sorted by Net Present Cost (NPC).

### Resource and Load Data

In India the annual average global solar radiation is about 5 kWh/m<sup>2</sup> per day with about 2300-3200 sun-shine hours per year. 1 kWp of SPV generates 3.5-4.5 units (kWhr) per day. The space requirement of SPV is 12-13 m<sup>2</sup>/kWp. Fig. 4 shows the monthly average daily solar radiation data and clearness index for Kolkata city in India [16]. Monthly average ambient temperature (°C) and sunshine hours are also illustrated in Fig. 5 [16].

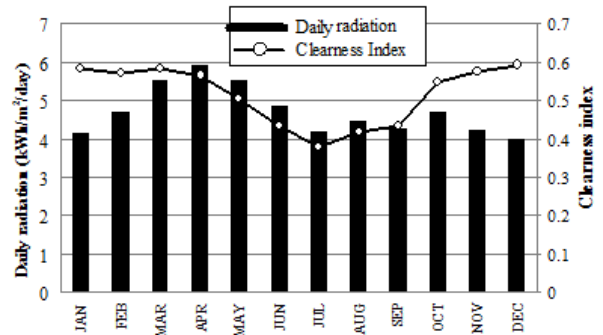


Fig. 4. Annual solar radiation profile [16]

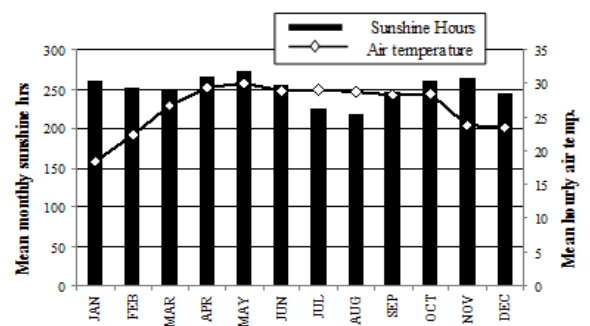


Fig. 5. Annual ambient temperature and sunshine hours [16]

The total DC power drawn by a shared (more than one service providers) Base Transceiver Station (BTS) at a telecom site is around 2 kW [17]. Generally, the service providers at a shared BTS site use a common grid connection and Diesel Generator (DG) set is provided by the infrastructure provider. The power plant and batteries are individually installed by the service providers. The use of renewable energy systems i.e. SPV can be efficiently utilized, if they are also provided centrally like the DG set. This reduces the overall system cost and requirement of the BTS site area. An electric hourly load profile with an average demand of 49.8 kWh/day, 4.2 kW peak demand and 2.1 kW average demand is obtained through HOMER electric load database and is shown in Fig. 6.

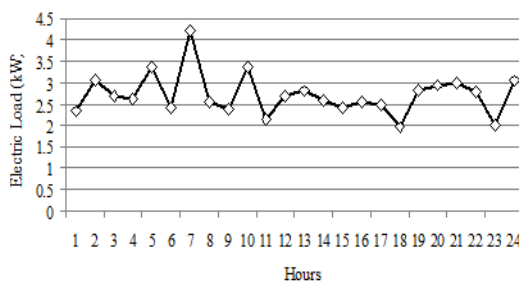


Fig. 6. Hourly load profile [15]

### Simulation Results

Three stand-alone SPV power system configurations using different hybrid energy storage technologies, namely, SPV-FC (System-I), SPV-Battery (System-II) and SPV-FC-Battery (System-III) are simulated using system model developed in Section II. Simulation is performed in HOMER environment for sizing optimization which minimizes the system cost. Simulation results also provide comparison among these configurations.

Cost, efficiency and lifetime of all major components are shown in Table I [12]. SPV<sub>T</sub> is representing the SPV system with MPPT having extra initial cost of 600\$. Simulation studies are classified as Case A, where all three system configurations are simulated without MPPT and Case B, where all three system configurations are simulated with MPPT in SPV.

**1) Case A:** Three different configurations of SPV power system without MPPT have been analyzed and compared in this case. Table II gives a comparison of components' optimal size, the Net Present Cost (NPC), the Cost of Electricity (COE) and the operating cost for all three system configurations. There is a huge gap between cost parameters of System I with other configurations. It is clear from this table that battery is economically a better choice for energy storage. The primary reason for this is the low efficiency of the FC/electrolyzer system. In fact, it is found that even if the capital costs of fuel cell and electrolyzer are reduced to half, the battery system is still an economically superior configuration. System II and III configurations are economically at par because of very small size of FC/electrolyzer system in optimal configuration.

TABLE I  
DETAILS OF SYSTEM COMPONENTS [13]

| Component            | Capital cost               | Replacement cost | Efficiency (%) | Lifetime |
|----------------------|----------------------------|------------------|----------------|----------|
| SPV                  | 6600 (\$/kW)               | 5000 (\$/kW)     | 14             | 20 yr    |
| SPV <sub>T</sub>     | 600 (\$) +<br>6630 (\$/kW) | 5028 (\$/kW)     | 14             | 20 yr    |
| FC                   | 2500 (\$/kW)               | 466 (\$/kW)      | 47             | 5 yr     |
| Battery              | 288 (\$/kWh)               | 216 (\$/kWh)     | 90             | 1 yr     |
| Electrolyzer         | 1000 (\$/kW)               | 466 (\$/kW)      | 74             | 10 yr    |
| H <sub>2</sub> tanks | 990 (\$/kWh)               | 500 (\$/kWh)     | 100            | 2 yr     |

TABLE II  
OPTIMAL SIZE AND COST PARAMETERS IN CASE A

| Configuration | Optimal size   | Total NPC (\$) | COE (\$/kWh) | Operating cost (\$/yr) |
|---------------|--|----------------|--------------|------------------------|
| System I      | SPV 160 kW<br>FC 4 kW<br>Electrolyzer 134 kW<br>H <sub>2</sub> Tanks 126 kg                    | 1792622        | 7.721        | 37995                  |
| System II     | SPV 21 kW<br>Battery 297.6 kWh   | 174312         | 0.904        | 2775                   |
| System III    | SPV 21 kW<br>Battery 297.6 kWh<br>FC 1 kW<br>Electrolyzer 1 kW<br>H <sub>2</sub> Tanks 0.25 kg | 177812         | 0.920        | 2794                   |

TABLE III  
ANNUALIZED ENERGY CONSUMPTION IN CASE A

| Configuration | Excess electricity (kWh/yr) | Capacity shortage (kWh/yr) | Unmet load (kWh/yr) |
|---------------|-----------------------------|----------------------------|---------------------|
| System I      | 44076                       | 18.2                       | 14.0                |
| System II     | 10221                       | 17.7                       | 15.1                |
| System III    | 8815                        | 17.7                       | 15.1                |

Table III shows annualized energy consumption for all three configurations. System III with two energy storage devices is producing least excess electricity, where as FC storage configuration (System I) has highest. However, all there configurations have capacity shortage and unmet load in the same range based on there optimal size of all components and load pattern.

**2) Case B:** Impact of MPPT has been analyzed in this case with all three system configurations. Optimal size of each component of the system and corresponding cost parameters for each SPV power system with MPPT ( $SPV_T$ ) is illustrated in Table IV. As the power point tracker enhances the SPV system efficiency, the optimal size of the SPV array is less compared to Case A and therefore all the corresponding cost parameters. Following the reasons given in Case A, cost parameters of System I has enormous variation with other configurations in Case B also.

Annualized energy consumption for all three system configurations is demonstrated in Table V. Compared to Case A, excess electricity produced is much higher with system configurations II and III because difference in optimal size of system components is manifested in System I configuration only.

TABLE IV  
OPTIMAL SIZE AND COST PARAMETERS IN CASE B

| Config uration | Optimal size         | Total NPC (\$) | COE (\$/kWh) | Opera ting cost (\$/yr) |
|----------------|----------------------|----------------|--------------|-------------------------|
| System I       | $SPV_T$              | 129 kW         | 6.653        | 39534                   |
|                | FC                   | 4 kW           |              |                         |
|                | Electrolyzr          | 130 kW         |              |                         |
|                | H <sub>2</sub> Tanks | 122 kg         |              |                         |
| System II      | $SPV_T$              | 19 kW          | 0.672        | 2654                    |
|                | Battery              | 307.2 kWh      |              |                         |
| System III     | $SPV_T$              | 19 kW          | 0.706        | 2674                    |
|                | Battery              | 307.2 kWh      |              |                         |
|                | FC                   | 1 kW           |              |                         |
|                | Electrolyzr          | 1 kW           |              |                         |
|                | H <sub>2</sub> Tanks | 0.25 kg        |              |                         |

TABLE V  
ANNUALIZED ENERGY CONSUMPTION IN CASE B

| Configuration | Excess electricity (kWh/yr) | Capacity shortage (kWh/yr) | Unmet load (kWh/yr) |
|---------------|-----------------------------|----------------------------|---------------------|
| System I      | 51947                       | 18.0                       | 13.9                |
| System II     | 15276                       | 15.4                       | 12.8                |
| System III    | 13557                       | 15.4                       | 12.8                |

### Sensitivity Analysis

The sensitivity of the effect of solar radiation on SPV arrays optimal size, cost parameters (NPC, COE and operating) of complete system and annualized energy consumption pattern is presented in Tables VI and VII.

As the annual average solar radiation is increased from 4 to 6 kWh/m<sup>2</sup>/day the optimal size of SPV arrays decreases and accordingly the cost of electricity and operating cost are also decreasing. In fact, with the change in resource values the system components optimal size varies that leads to different system cost parameters. In Table VII, excess electricity produced regularly increases with increase in the annual average solar radiation; however capacity shortage and unmet load have no definite pattern because of irregular nature of load profile.

TABLE VI  
COST SENSITIVITY ANALYSIS

| Annual average radiation (kWh/m <sup>2</sup> /day) | SPV (kW) | Total NPC (\$) | COE (\$/kWh) | Operating cost (\$) |
|--|----------|----------------|--------------|---------------------|
| 4  | 23       | 233255         | 1.005        | 3074                |
| 4.5  | 21       | 215010         | 0.926        | 2864                |
| 4.7  | 20       | 209494         | 0.902        | 2861                |
| 5  | 19       | 165138         | 0.863        | 2756                |
| 5.5  | 18       | 189446         | 0.816        | 2600                |
| 6  | 17       | 181193         | 0.780        | 2564                |

TABLE VII  
ENERGY SENSITIVITY ANALYSIS

| Annual average radiation (kWh/m <sup>2</sup> /day) | Excess electricity (kWh/yr) | Capacity shortage (kWh/yr) | Unmet load (kWh/yr) |
|--|-----------------------------|----------------------------|---------------------|
| 4  | 7626                        | 18.1                       | 15.4                |
| 4.5  | 8775                        | 17.0                       | 14.3                |
| 4.7  | 8740                        | 16.7                       | 14.1                |
| 5  | 9139                        | 18.1                       | 15.5                |
| 5.5  | 10135                       | 14.6                       | 12.3                |
| 6  | 9749                        | 16.1                       | 13.8                |

### Discussion And Conclusion

Renewable hybrid SPV power systems using different energy storage technologies have been modeled, optimized and compared using HOMER software in this work. Effect of using MPPT system with all three SPV system configurations has also been analyzed.

Although this study shows that hydrogen energy storage system is economically slightly less competitive with battery storage systems, there are other benefits to hydrogen storage system worth mentioning like environment friendlier (no ecological cost is associated) and increase in storage size is cheaper compared to batteries. Therefore, among three SPV system configurations, SPV-FC-Battery hybrid system acquires the configuration with the lowest system cost (including battery environmental cost) and best energy consumption pattern as compared with either single storage system. Further application of MPPT reduces the optimal number of SPV arrays and therefore overall system cost and improves the system performance.

In future, the work on detailed economic analysis of the hardware based on availability of solar resource and simulation of controller and hardware implementation will be reported.

### Acknowledgment

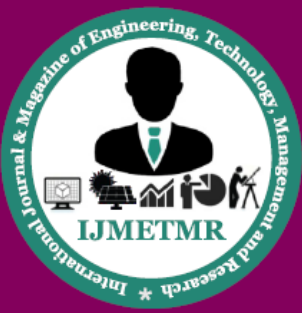
Authors are thankful to authorities of ssn engg college ongole for the encouragement in this work and permission to publish the paper.

### References

1. T. Markvart, "Sizing of hybrid photovoltaic-wind energy systems," *Solar Energy*, vol.57, No.4, pp.277-281, 1996.
2. P. A. Lehman, C. E. Chamberlin, G. Pauletto, and M. A. Rocheleau, "Operating experience with a photovoltaic-hydrogen energy system," *Proceedings, Hydrogen '94: The 10th World Hydrogen Energy Conference*, Cocoa Beach, Florida, June, 1994.
3. R. Ramakumar, I. Abouzahar, and K. Ashenayi, "A

knowledge based approach to the design of integrated renewable energy systems," *IEEE Trans. Energy conversion*, vol. 7, pp. 648-659, Dec. 1992.

4. Kaushik Rajashekara, "Hybrid Fuel Cell strategies for clean power generation," *IEEE Transactions on Industry Applications*, vol. 41, No. 3, pp.682-689, May/June 2005.
5. Th. F. El-Shatter, M. N. Eskandar, and M. T. El-Hagry, "Hybrid PV/Fuel Cell system design and simulation," *Renewable Energy*, vol. 27, No. 3, pp.479-485, November 2002.
6. A. Dmowski, P. Biczal, and B. Kras, "Stand-alone telecom power system supplied by PEM fuel cells and renewable sources," *International Fuel Cell workshop*, Kofu, Japan, 2001.
7. D. B. Nelson, M. H. Nehrir, and C. Wang, "Unit sizing of stand-alone hybrid wind/PV/fuel cell power generation systems," *IEEE Power Engineering Society General Meeting*, vol. 3, June 2005, pp. 2116- 2122.
8. M. S. Alam, and D. W. Gao, "Design, modeling and analysis of a hybrid applications," *Global conference on Renewable Energy Approaches for Desert Regions*, Amman, Jordan, September, 2006.
9. J. D. Maclay, J. Brouwer, and G. S. Samuelsen, "Dynamic modeling of hybrid energy storage systems coupled to photovoltaic generation in residential applications," *Power Sources*, vol. 163, No.2, pp.916-25, 2006.
10. M. Santarelli, and D. Pellegrino, "Mathematical optimization of a RES-H2 plant using a black box algorithm," *Renewable Energy*, vol. 30, No. 4, pp.493-510, 2005.
11. W. D. Johnston, *Solar voltaic cells*, Ist ed., New York: Marcel Dekker, 1980.
12. J. Larminie, and A. Dicks, *Fuel cell systems*



explained. 2nd ed. England: Wiley: 2003.

13. Leonidas Ntziachristos, Chariton Kouridis, Zissis Samaras and Konstantinos Pattas, "A wind–power fuel-cell hybrid system study on the non-interconnected Aegean islands grid," Science direct, vol. 30, pp. 1471-1487, Dec. 2004.

14. M. J. Khan and M. T. Iqbal, "Dynamic modeling and simulation of a small wind-fuel cell hybrid energy system," Renewable Energy, pp.421-439, 2005.

15. Home page of HOMER, Available: <http://www.nrel.gov/homer/>.

16. Solar Radiation Hand Book, 2008, A joint Project of Solar Energy Centre, MNRE and Indian Metrological Department, Available: <http://mnes.nic.in/sec/srd-sec.pdf>

17. Hybrid wind/solar power for rural telephony: Green solution to power problems, 2008, DOT committee report on renewable energy, Availble : [www.dot.gov.in/finstatus/Telecom Manual.pdf](http://www.dot.gov.in/finstatus/Telecom Manual.pdf)